2-3D NUMERICAL MODEL OF JET FORMATION IN SOLAR ATMOSPHERE

J. J. GONZÁLEZ-AVILÉS[1], F. S. GUZMÁN[1], V. FEDUN[2], G. VERTH[3], S. SHELYAG[4] AND S. REGNIER[4]

[1]INSTITUTO DE FÍSICA Y MATEMÁTICAS, UNIVERSIDAD MICHOACANA DE SAN NICOLÁS DE HIDALGO. MORELIA, MICHOACÁN, MÉXICO

[2]DEPARTMENT OF AUTOMATIC CONTROL AND SYSTEMS ENGINEERING, UNIVERSITY OF SHEFFIELD, SHEFFIELD, UK

[3]SCHOOL OF MATHEMATICS AND STATISTICS, UNIVERSITY OF SHEFFIELD, UK

[4]DEPARTMENT OF MATHEMATICS, PHYSICS AND ELECTRICAL ENGINEERING, NORTHUMBRIA UNIVERSITY, NEWCASTLE UPON TYNE, UK

AOGS
AUGUST 6-11, 2017
SINGAPORE

OUTLINE

- Resistive MHD equations
- Numerical methods
- Model of the solar atmosphere
- Magnetic field configurations
  - 2D magnetic loops.
  - 3D extrapolated magnetic configuration.
- Results of numerical simulations
  - 2D: Symmetric, non-symmetric configurations and Kelvin-Helmholtz instability feature.
  - 3D: Evolution of temperature, upward velocity, dominant forces, vorticity and Doppler shift.
- Final comments

RESISTIVE MHD EQUATIONS

Extended Generalized Lagrange Multiplier (EGLM) resistive MHD equations with gravity

Newtonian CAFE code
*González-Avilés J.J., et al. 2015, MNRAS, **454**,1871*

$$\frac{\partial \rho}{\partial t} + \nabla \cdot (\rho \mathbf{v}) = 0,$$

$$\frac{\partial (\rho \mathbf{v})}{\partial t} + \nabla \cdot \left(\left(p + \frac{1}{2}\mathbf{B}^2 \right) \mathbf{I} + \rho \mathbf{v}\mathbf{v} - \mathbf{B}\mathbf{B} \right) = -(\nabla \cdot \mathbf{B})\mathbf{B} + \rho \mathbf{g},$$

$$\frac{\partial E}{\partial t} + \nabla \cdot \left(\mathbf{v} \left(E + \frac{1}{2}\mathbf{B}^2 + p \right) - \mathbf{B}(\mathbf{B} \cdot \mathbf{v}) \right) = -\mathbf{B} \cdot (\nabla \psi) - \nabla \cdot ((\eta \cdot \mathbf{J}) \times \mathbf{B}) + \rho \mathbf{g} \cdot \mathbf{v},$$

Ohmic dissipation

$$\frac{\partial \mathbf{B}}{\partial t} + \nabla \cdot (\mathbf{B}\mathbf{v} - \mathbf{v}\mathbf{B} + \psi \mathbf{I}) = -\nabla \times (\eta \cdot \mathbf{J}),$$

Diffusion

$$\frac{\partial \psi}{\partial t} + c_h^2 \nabla \cdot \mathbf{B} = -\frac{c_h^2}{c_p^2} \psi.$$

NUMERICAL METHODS

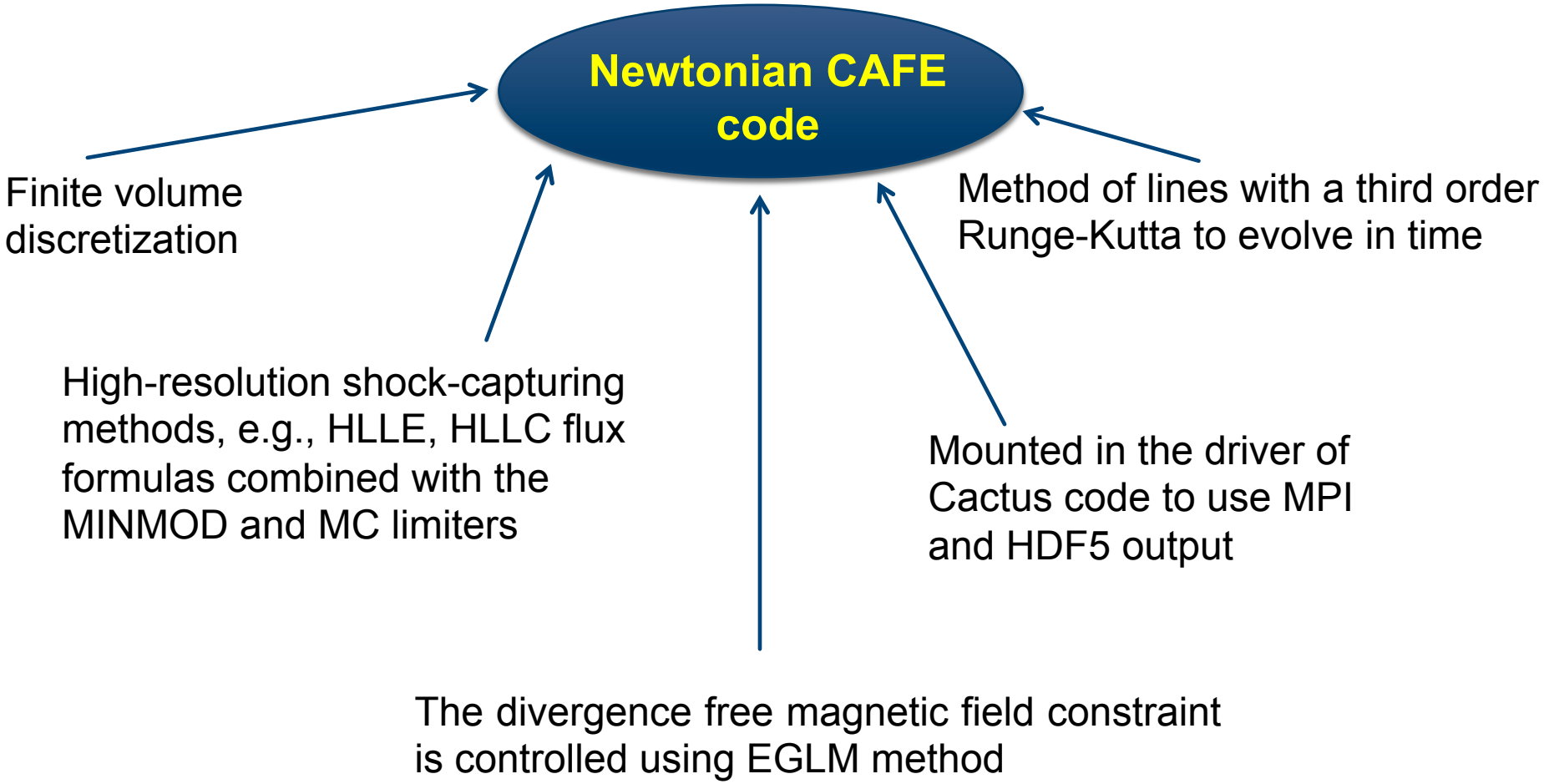

MODEL OF THE SOLAR ATMOSPHERE

The solar atmosphere in hydrostatic equilibrium is given by the C7 model (*Avreet E. H & Loeser R. 2008, ApJS, **175**, 229*).

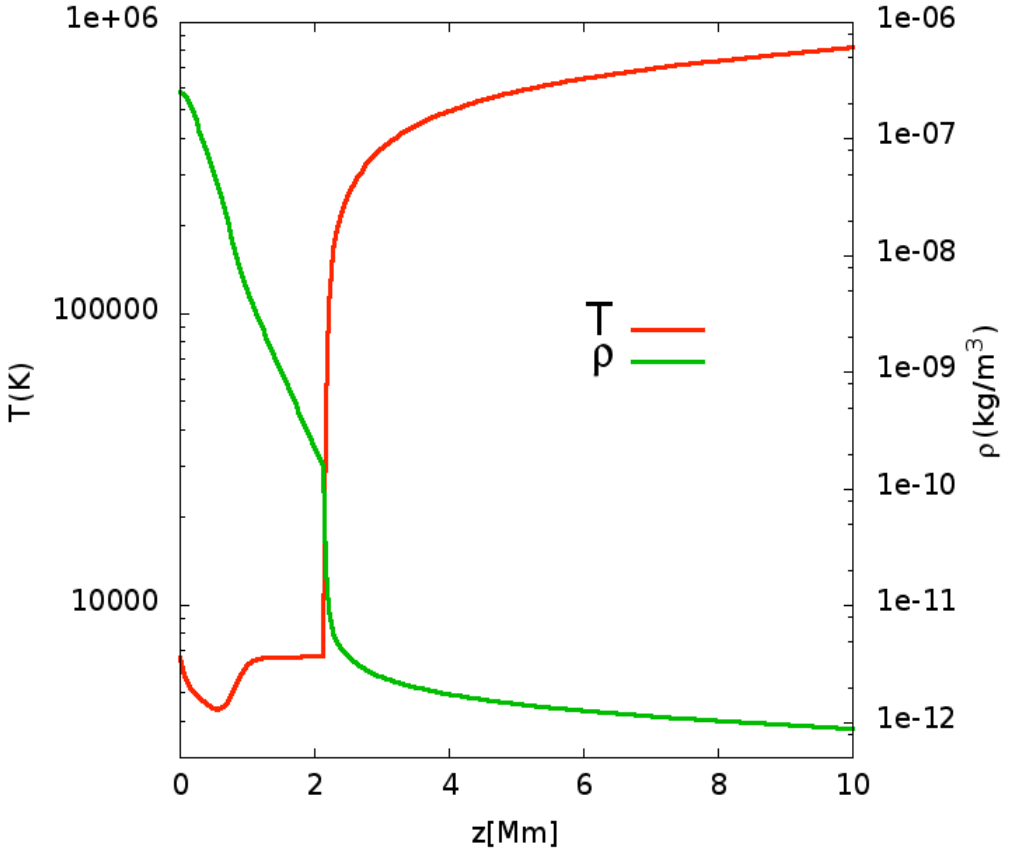

Temperature (red) and mass density (green) as a function of z

MAGNETIC FIELD CONFIGURATIONS

2D magnetic loops

$$A_y(x,z) = \frac{B_{01}}{k}\cos(k(x+l_0))\exp(-kz) + \frac{B_{02}}{k}\cos(k(x-l_0))\exp(-kz), \quad k = L/\pi$$

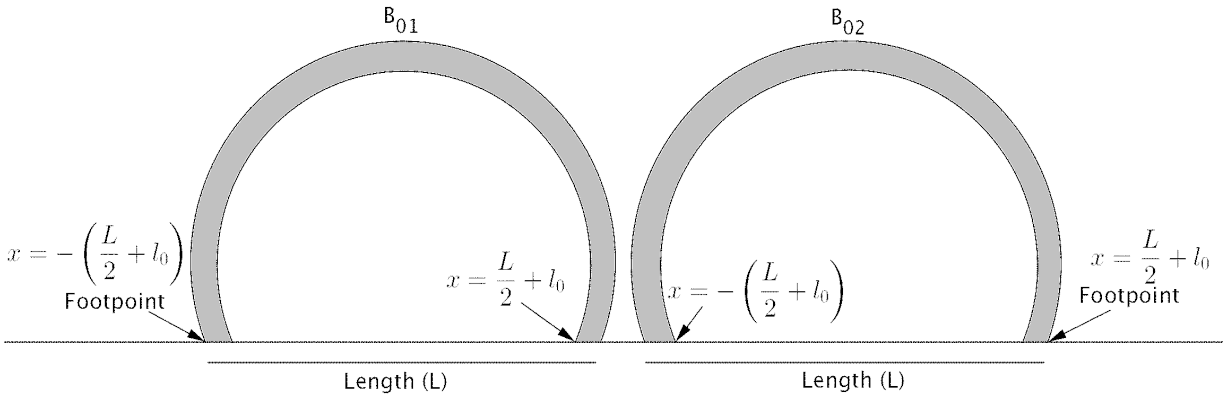

Symmetric configurations

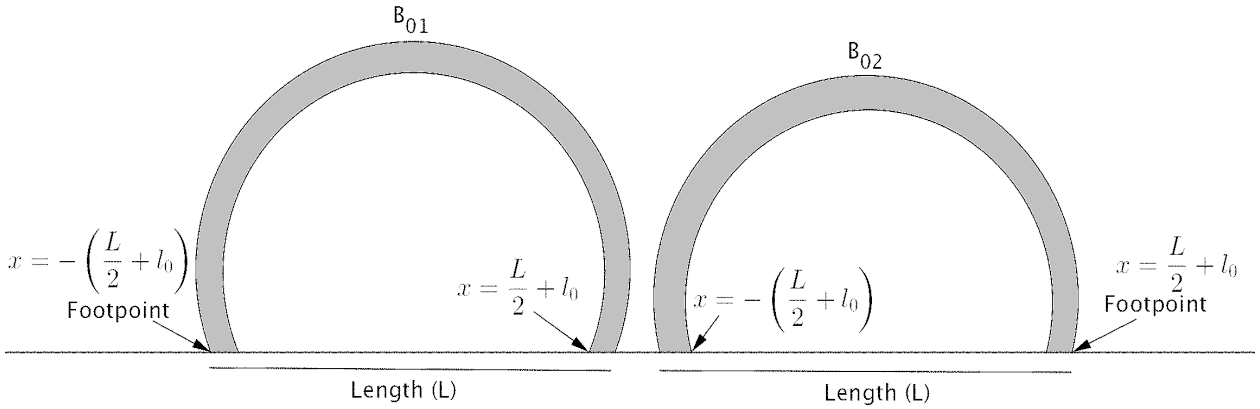

Non-symmetric configurations

RESULTS OF NUMERICAL SIMULATIONS

Symmetric configurations

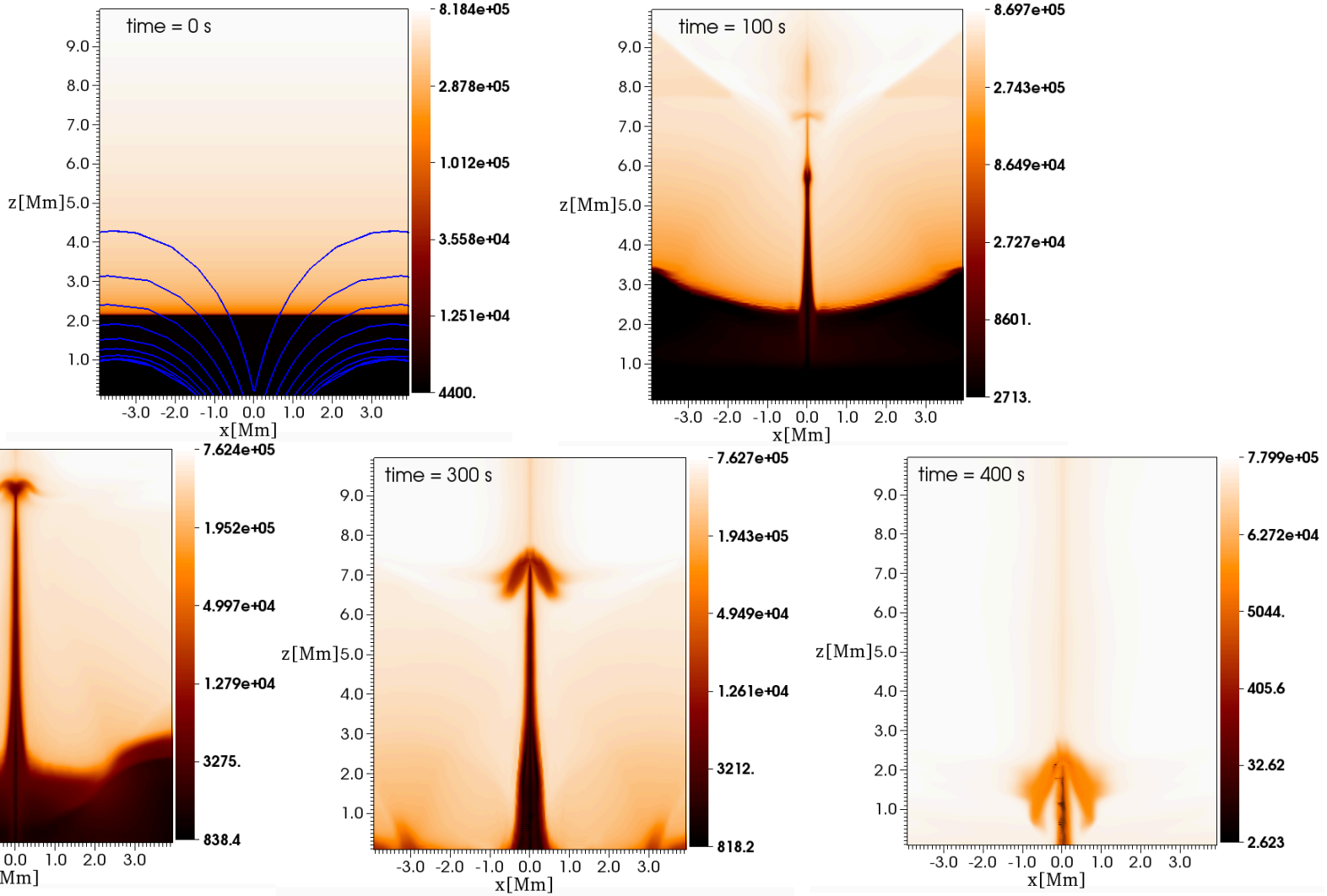

Snapshots of the temperature for the case $B_{01}=B_{02}=40$ G and $l_0=3.5$ Mm.

Non-symmetric configurations

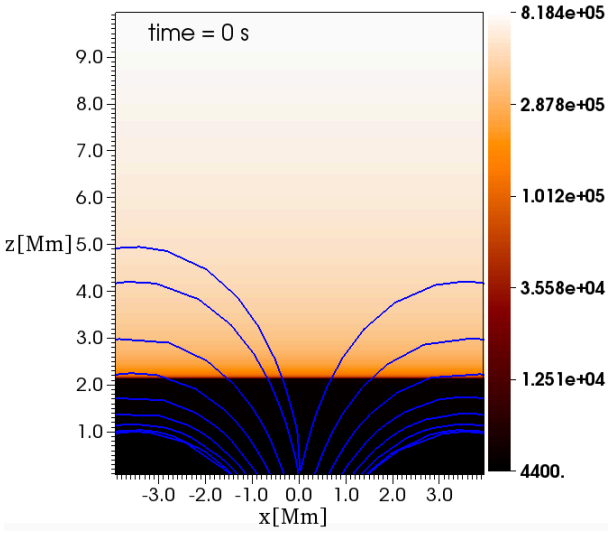

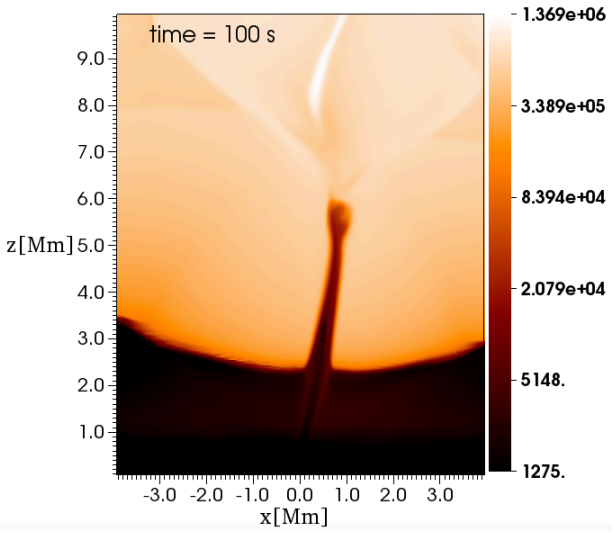

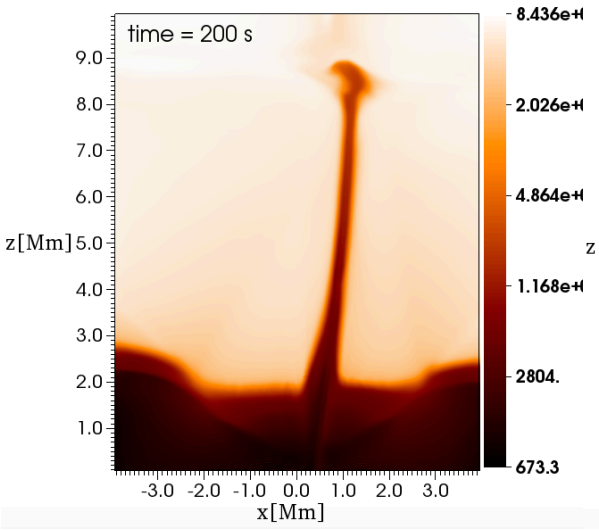

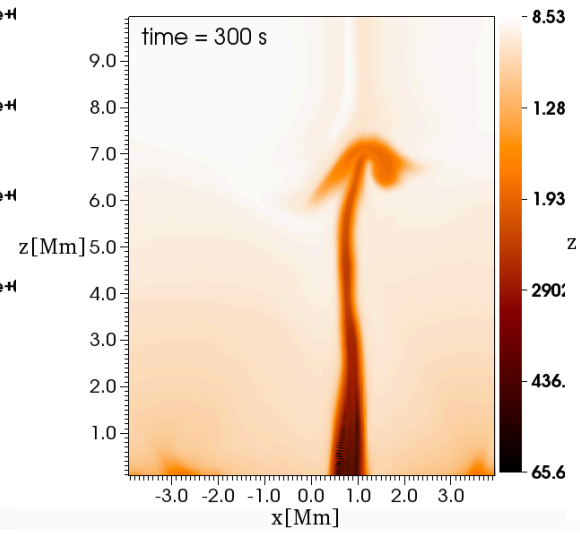

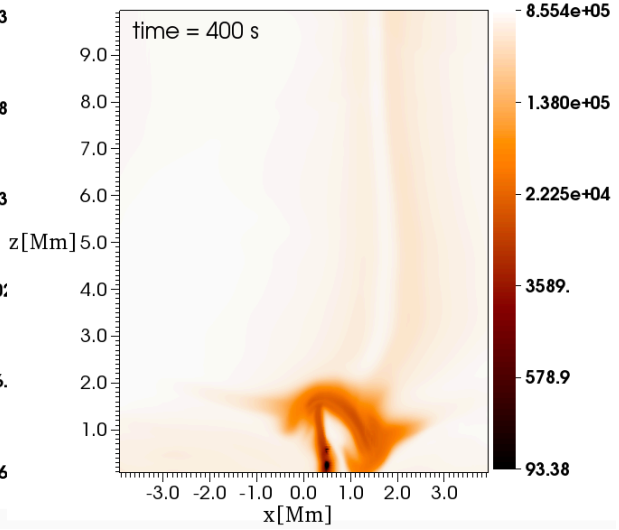

Snapshots of the temperature for the case B_{01}=40 G, B_{02}=30 G and l_0=3.5 Mm.

Kelvin-Helmholtz Instability feature

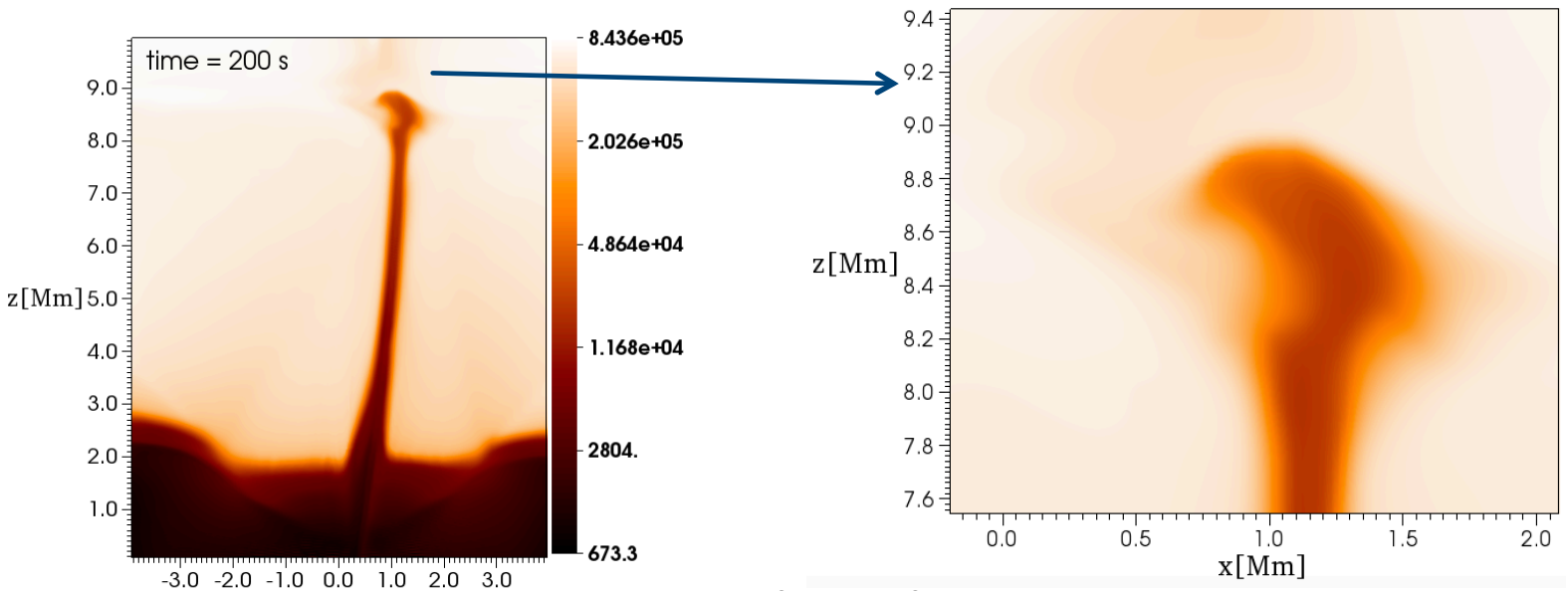

$$\frac{B_z^{(-)^2}+B_z^{(+)^2}}{\mu_0\rho^{(+)}\rho^{(-)}}(\rho^{(+)}+\rho^{(-)}) \geq (v_z^{(-)}-v_z^{(+)})^2$$

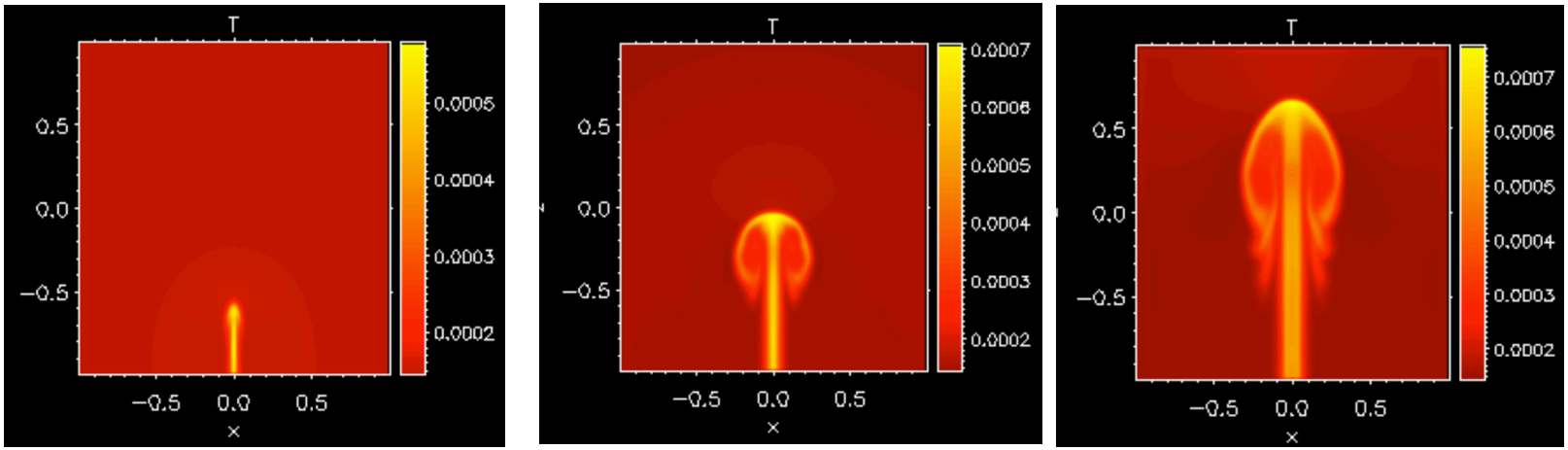

Temperature for a hydrodynamic jet

3D extrapolated magnetic configuration

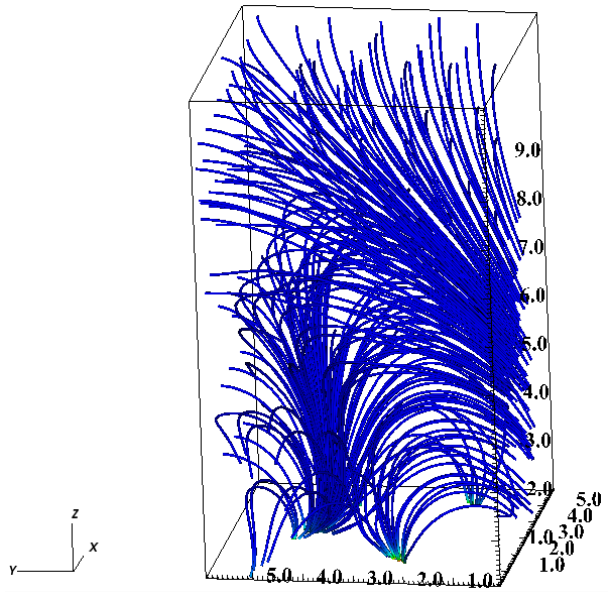

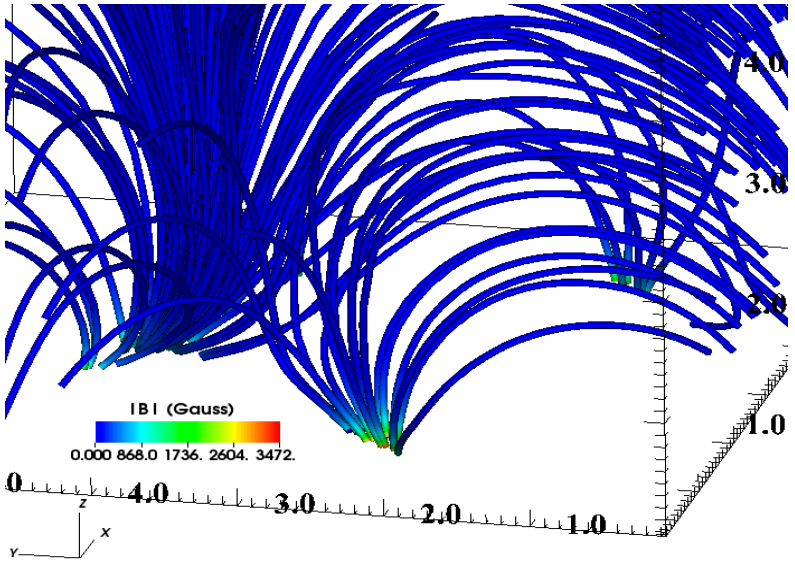

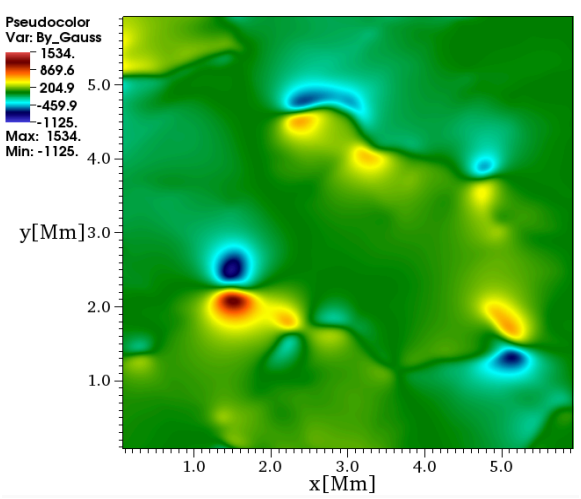

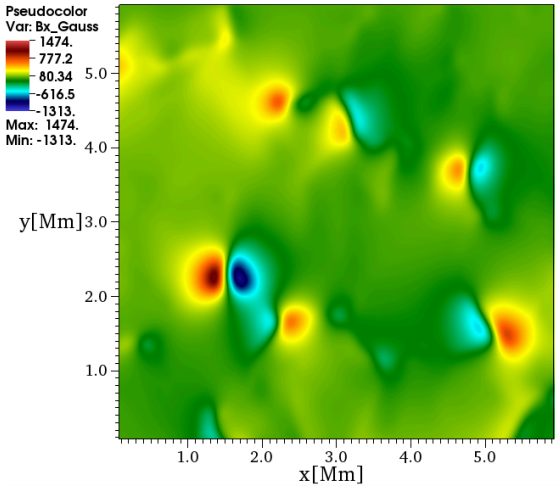

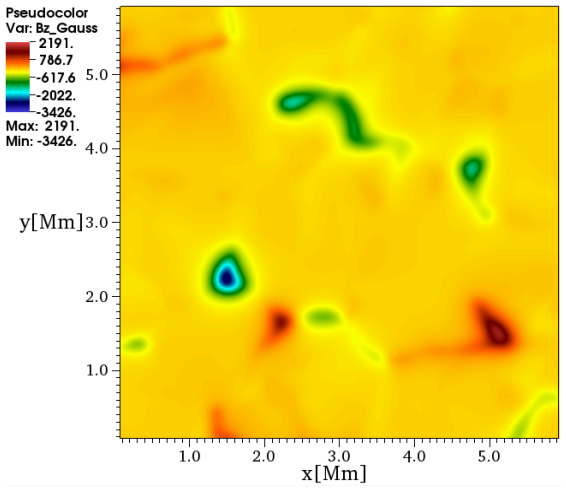

(Top) Magnetic field lines and zoom of strong bipolar regions in the 3D domain at initial time. (Bottom) Three components of the magnetic field B_x, B_y and B_z at the plane z = 0.1Mm. The color bars represent the magnitude of the magnetic field in Gauss.

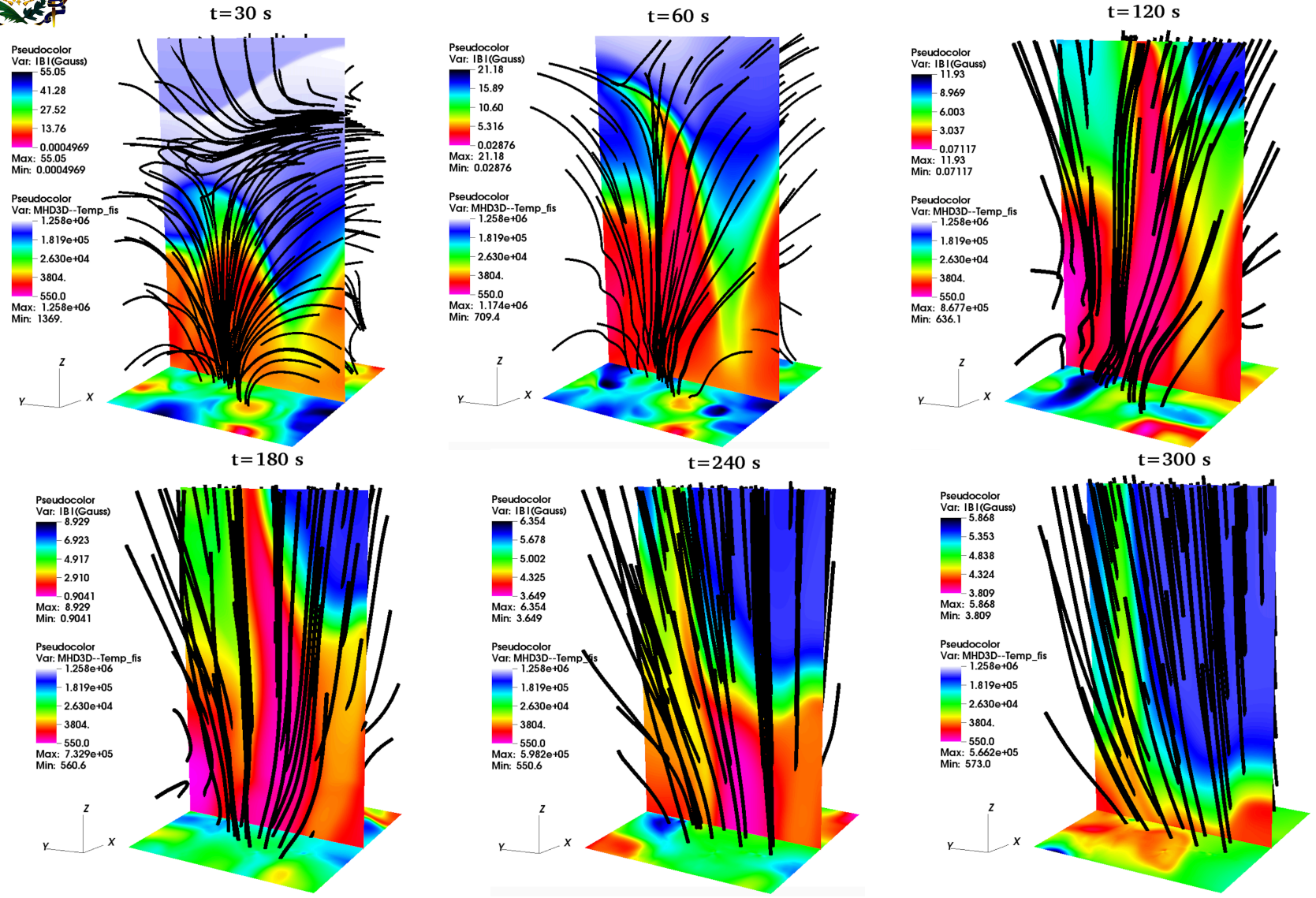

Snapshots of the temperature (K) and magnetic field lines in 3D (black) at 30, 60, 120,180, 240 and 300 s.

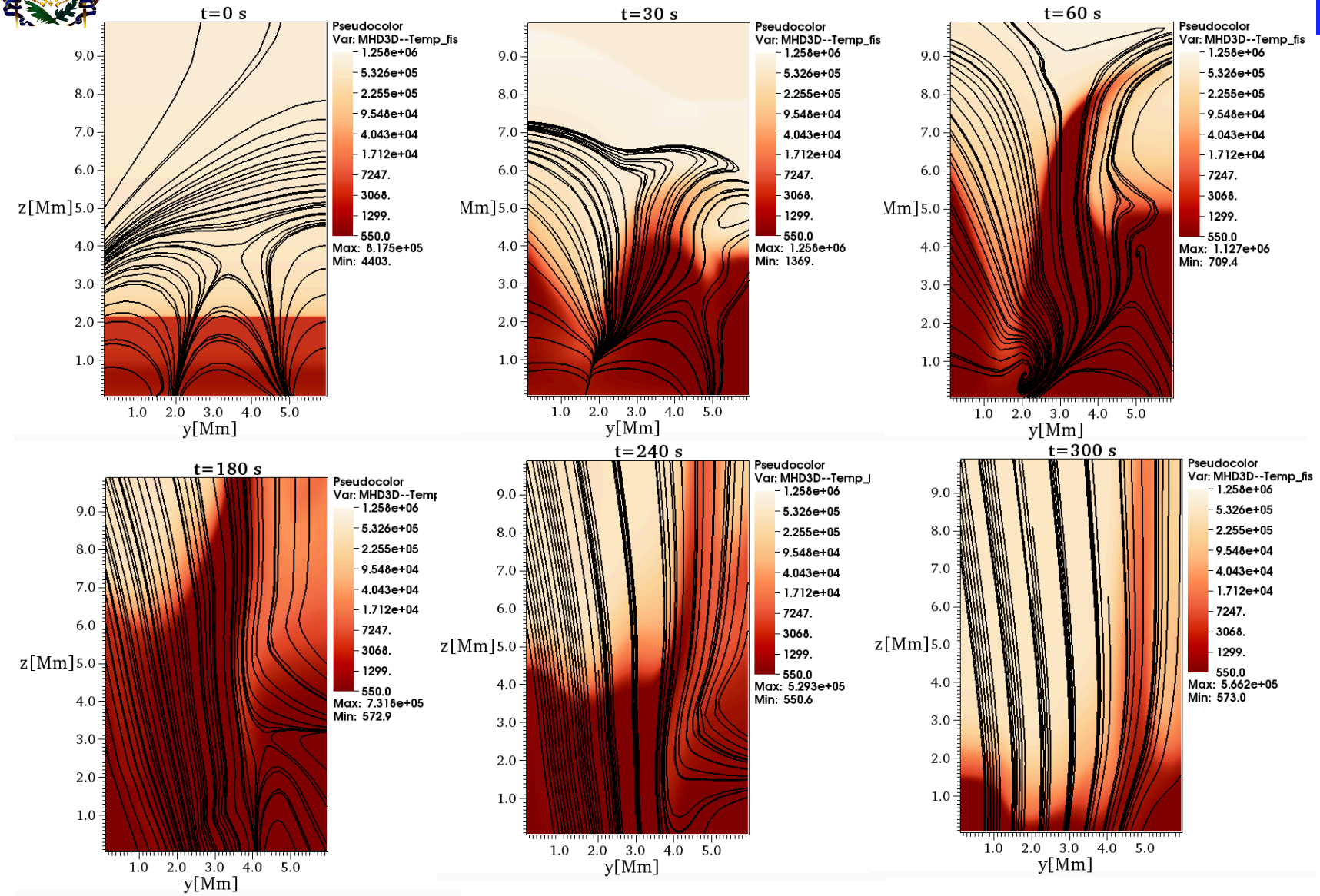

Snapshots of the temperature (K) and magnetic field lines in the cross cut at the plane x =0.1 Mm at times 30, 60, 120, 180, 240 and 300 s.

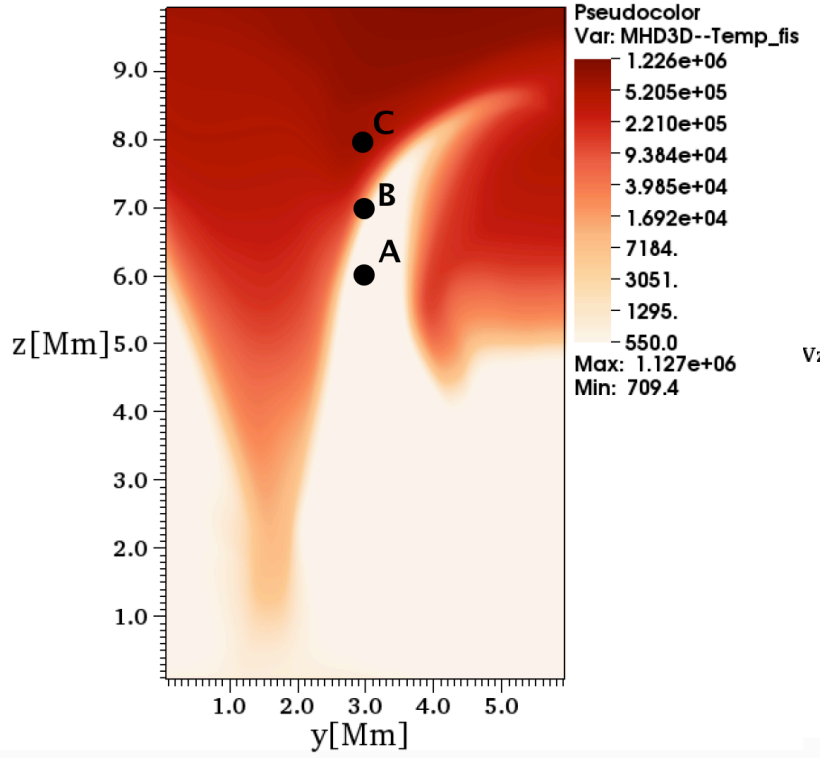

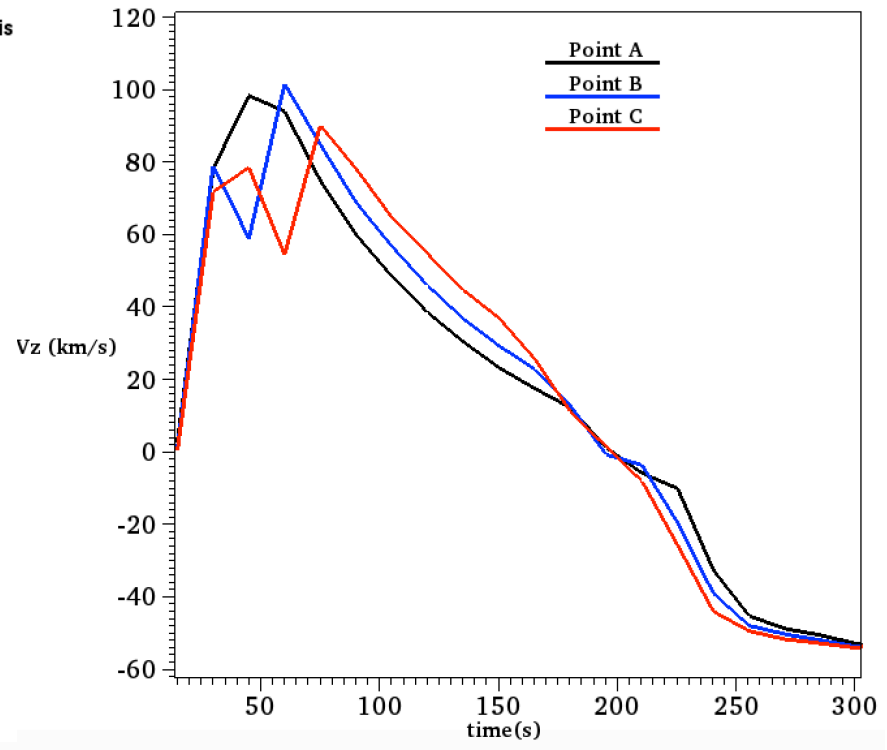

(Left) Logarithm of temperature in the yz plane at x =0.1 Mm at time t = 60 s and (right) time series of v_z in km s^{-1} measured at points A, B and C.

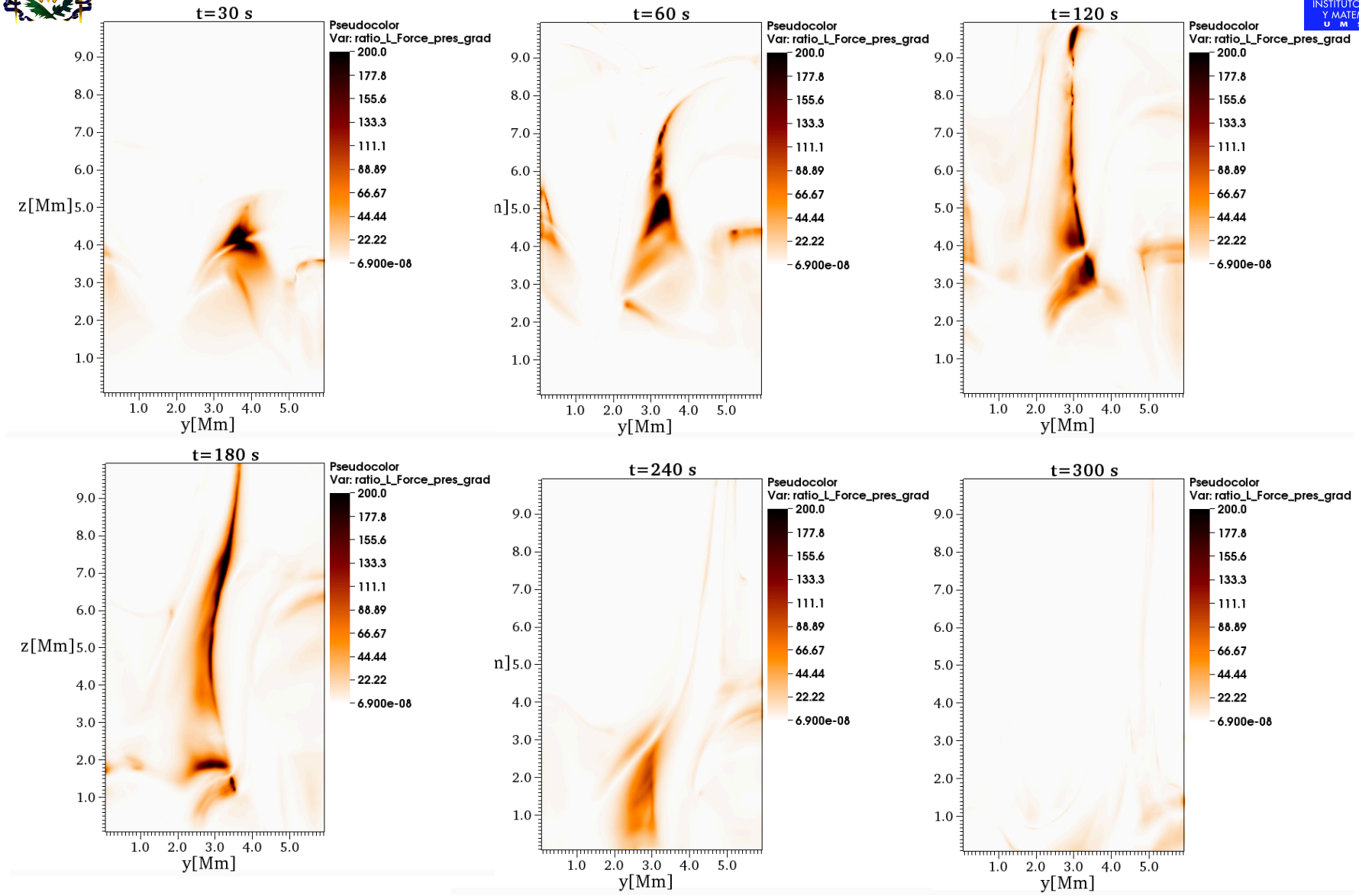

Snapshots of the ratio $|\mathbf{J} \times \mathbf{B}|/|\nabla p|$ in the cross cut at the plane x = 0.1 Mm at various times.

Vorticity and Doppler shift

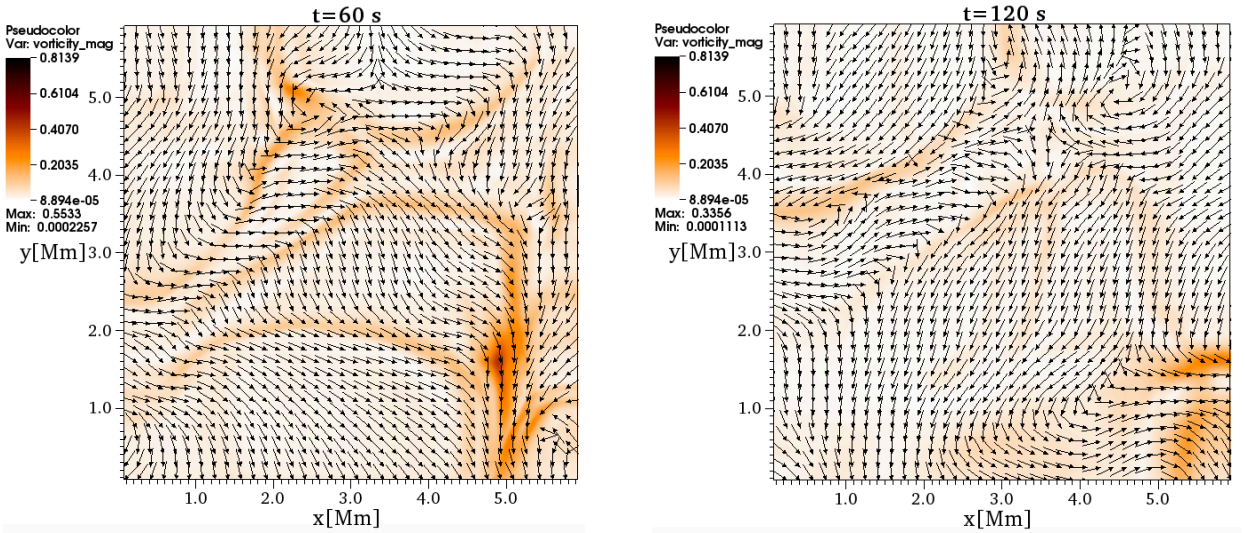

Snapshots of the magnitude of the vorticity |ω| in s-1 and vector velocity field in the plane z = 3.5 Mm.

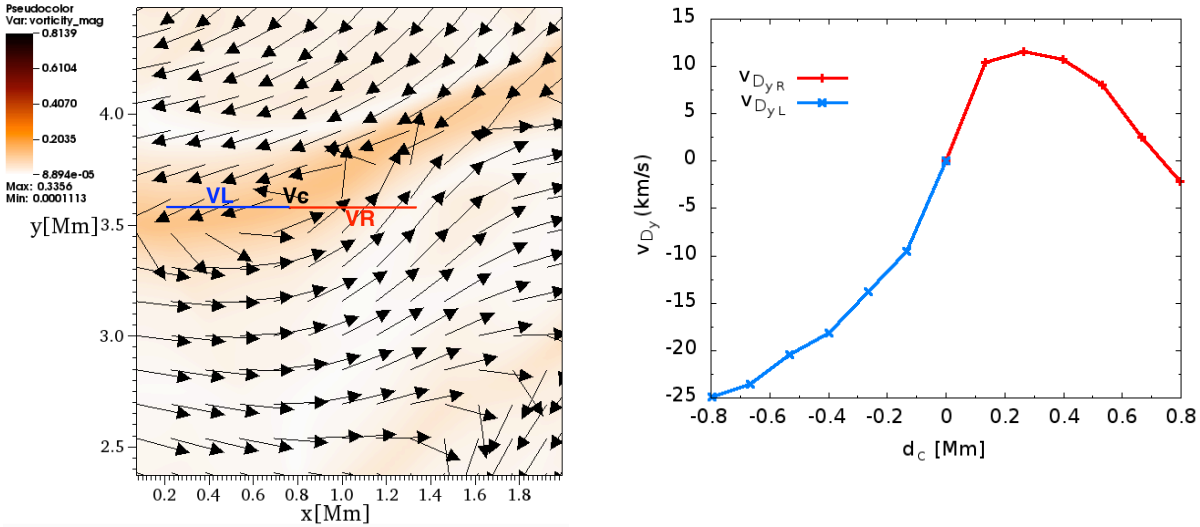

(Left) Region where the Doppler shift v_{Dy} is estimated. (Right) Value of v_{Dy} of the y component of velocity v_y or equivalently the tangent velocity as a function of distance from the center.

FINAL COMMENTS

- In the case of the 2D simulations, we use an idealized model to show that jets with features of type II spicules and cool coronal (10^4 K) can be formed due to magnetic reconnection using a value of resistivity $\eta=10^{-2}$ Ω m and present a Kelvin-Helmholtz type instability (*González-Avilés, J.J., Guzmán, F. S., & Fedun, V. 2017, ApJ,* ***836****, 24*).

- In the 3D case, we use a potential magnetic field, extrapolated up to the corona region obtained from a realistic simulation of solar photospheric magnetoconvection model to show that magnetic reconnection can be responsible of the formation of a jet with similar characteristics of a type II spicule (*González-Avilés, J.J. et al. 2017, ApJ,* ***submitted***).
  - The formation of this jet depends on the Lorentz force.
  - The jet structure shows Doppler shift near to regions with high vorticity.
  - The upward velocity of the jet is of the order 100 km s^{-1} and the life-time longer than 100 s.